A novel change detection method of multi-resolution remotely sensed images based on the decision level fusion

LIU Sicong[1], DU Peijun[1, 2], CHEN Shaojie[2]

1. *Key Laboratory for Land Environment and Disaster Monitoring of SBSM*, *China University of Mining and Technology*, *Jiangsu*, *Xuzhou* 221116, *China*;
2. *College of Resources Engineering*, *Longyan University*, *Fujian Longyan* 364000, *China*

Abstract: According to the characteristics and merits of multi-resolution remotely sensed images and objectives of different change detection applications, the idea using coarse to fine (CTF) hierarchical detection and decision level fusion are introduced into change detection process. The technical flow of change detection based on CTF is designed and implemented with multi-temporal ALOS images as the experimental data. The four band ALOS multi-spectral images are viewed as coarse resolution data, and the panchromatic image and fusion image of multispectral and panchromatic data are viewed as fine data. After processing the fine and coarse datasets individually, results are integrated to form a new dataset which reflects the location and intensity of final changes based on specific fusion rules. Land cover change detection of two study case areas over the urban area and mining area of Xuzhou City are conducted. Comparing the proposed approach with other common methods, it is concluded that the proposed CTF decision level fusion change detection approach outperforms other traditional algorithms, and it is effective to conduct change detection using multi-resolution remotely sensed images, further providing the important target change areas of field work.

Key words: change detection, coarse to fine (CTF), decision level fusion, land cover change

CLC number: TP75 **Document code:** A

Citation format: Liu S C, Du P J and Chen S J. 2011. A novel change detection method of multi-resolution remotely sensed images based on the decision level fusion. *Journal of Remote Sensing*, **15**(4): 846–862

1 INTRODUCTION

Change detection plays an important role in remote sensing applications because multi-temporal imagery can reflect the change of the ground surface in a certain temporal interval. Typical application areas including land use/cover change, vegetation change, urban extension, disaster monitoring, *etc*. Change detection is the process of identifying differences in the state of an object or phenomenon by observing it at different time (Singh, 1989). For decades, a lot change detection techniques have been proposed utilizing the multi-temporal remotely sensed images. For binary change detection, conventional algorithms can be divided into two main categories: supervised and unsupervised algorithms. The former is similar to supervised classification, in which a suitable training set should be obtained to input into the detect module, for example, *post-classification comparison* (PCC), *artificial neural network* (ANN) and *support vector machines* (SVM) (Castellana, *et al.*, 2007; Nemmour & Chibani, 2006; Woodcock, *et al.*, 2001). The latter analy-ses and processes the original images directly to derive change information, for example, image differencing, image ratioing, *change vector analysis* (CVA), *principal component analysis* (PCA) and *object-oriented* approach (Bovolo & Bruzzone, 2007; Bruzzone & Prieto, 2000; Fung & LeDrew, 1987; Lambin & Strahler, 1994; Riordan, 1981; Sohl, 1999; Walter, 2004). Despite the methodological strengths of all these methods, there are still several problems in change detection technique that need to be considered. Firstly, all these methods have different applicability, some for single-band image detection, and some for multi-band image detection, indicating that there are no universally applicable high-precision algorithms. Secondly, the information contained in different resolution image data is different, especially for the multi-resolution image data with the same satellite. Generally, more spectral information is contained than that in multi-spectral image data, and sufficient texture information in panchromatic image data have great impacts on the results of change detection. Thirdly, change detection applications with different objectives have different demands for omission and commission detection ratios. How to focus on the specific application, and select the most suitable approach

Received: 2010-03-22; **Accepted:** 2010-06-20

Foundation: National High Technology Research and Development Program of China (No.2007AA12Z162); Natural Science Foundation of China (No.40871195) and "333 project" scientific research fund of Jiangsu province

First author biography: LIU Sicong (1986—), male, Graduate student, Department of Remote sensing and Geographical Information Science, China University of Mining and Technology. Current research field: remote sensing image processing and remote sensing application. E-mail: allencong@163.com

Corresponding author: DU Peijun (1975—), male, professor of remote sensing at University of Mining and Technology. His research interests are remote sensing image processing, pattern recognition, remote sensing applications in resources, environment and urban studies, integration and applications of geospatial information technologies. Email: dupjrs@126.com

in order to minimizing the omission or commission have not been extensively investigated.

Aiming to address the aforementioned problems, the CTF multi-resolution image processing, decision tree and decision level fusion theories are introduced into multi-temporal, multi-resolution remote sensing image change detection. According to the specific application of reducing omission and restraining commission, two novel change detection strategies based on decision level fusion are designed, and then results are compared with traditional algorithms in order to explore its feasibility and applicability. Unlike the definition of general coarse to fine theory, the proposed method in this paper focuses on the change detection from datasets with different resolution of multi-resolution remote sensing images. Combining the detection results from different resolution datasets and different approaches, this novel approach can take full advantage of their merits to avoid and reduce the uncertainty when using single change detection algorithm or single data source.

2 CHANGE DETECTION FROM MULTI-RESOLUTION IMAGES BASED ON COARSE TO FINE DECISION LEVEL FUSION

The theory of CTF is mainly used in pattern recognition fileds, such as face recognition and detection, mobile vehicles track detection and image shape detection (Atiquzzaman, 1999; Li, *et al.*, 2006; Sahbi, *et al.*, 2002). In remote sensing image processing domain, the CTF idea is also used in the processing of multi-scale images, especially for the panchromatic and multi-spectral image data of the same satellite. The proposed method makes full use of the characteristics and merits of different resolution datasets and different change detection approaches to detect the change location and define the change intensity by integrating multiple results. Then, areas which have the largest change intensity are further used as important target areas for field work. Meanwhile, two CTF fusion rules handling different practical applications are designed and experimented to maximize the reduction of omission rate and restrain of the commission rate, and finally to increase the overall accuracy of change detection.

Fig. 1 shows the flowchart of the novel approach proposed in this paper. According to the properties of ALOS data, two change detection strategies based on CTF fusion are designed and experimented. Detailed steps are described as follows.

Strategy 1:

(1)The multispectral (Ms) ALOS image data with 10 m spatial resolution is viewed as coarse data, and the panchromatic (Pan) image with 2.5 m spatial resolution is used as fine data. Then the change detection are conducted on the two datasets, respectively;

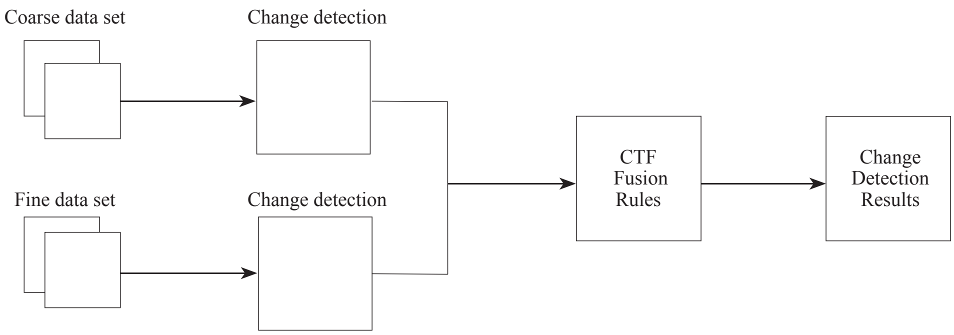

Fig. 1 Flowchart of the CTF change detection based on decision level fusion

(2)Resampling the two datasets change maps into the same resolution of 2.5 m;

(3)Combining the two change maps to form the final change intensity map based on the CTF fusion rule, and redefines all pixels into four groups: strong change (change occurs on both coarse and fine dataset), obvious change (change occurs only on coarse data set), subtle change (change only occurs on find data set) and unchanged.

Table 1 is a summary of change intensity redefinition, in which value 1 corresponds to changed pixels in the dataset and value 0 means unchanged. Fig. 2 illustrates the decision tree established according to the change intensity table, in which B1 and B2 represent results of fine dataset and coarse dataset, respectively.

Table 1 Definition of pixel change intensity

Dataset	Pixel value on change map			
Fine dataset (Pan)	1	0	1	0
Coarse dataset (Ms)	1	1	0	0
Change intensity	Strong change	Obvious change	Subtle change	Unchanged

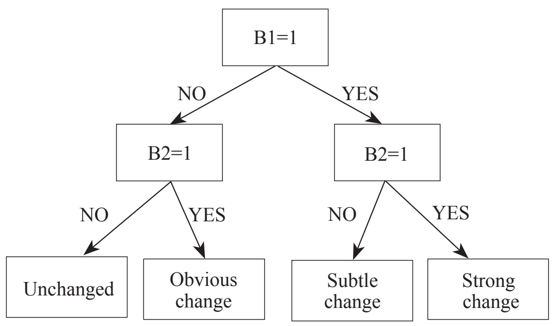

Fig. 2 Decision tree rule to define change intensity based on coarse and fine dataset (CTF strategy 1)

Strategy 2:

(1)The multispectral (Ms) ALOS image data is viewed as coarse data, the panchromatic (Pan) image and Fusion images of Ms and Pan are viewed as fine data. Then change detection are conducted on the three image data respectively;

(2)Resampling the three change maps from three datasets into the same resolution.

(3)Establishing the CTF fusion rule: strong change (change occurs on all three datasets), obvious change (change occurs on any two datasets), subtle change (change only occurs on one dataset) and unchanged. Finally, the former two groups are considered as change areas, and latter two are viewed as unchanged. Table 2 is the definition of all pixels change intensity.

Table 2 Definition of pixel change intensity

Dataset	Pixel value on change map							
Coarse dataset (Ms)	1	1	1	0	1	0	0	0
Fine dataset (Pan)	1	1	0	1	0	1	0	0
Fine dataset (Fusion)	1	0	1	1	0	0	1	0
Change intensity	Strong change		Obvious change			False alarms (Unchanged)		Unchanged

The error matrix or confusion matrix is used to derive related change detection accuracy indicators (Table 3).

Table 3 Error matrix of change detection

Detected data/ valiation data	True changes (c)	True unchanges (u)	Total
Detected changes(C)	Cc	Cu	TC
Detected unchanges(U)	Uc	Uu	TU
Total	Tc	Tu	T

Some common accuracy assessment indicators are also included:

● Overall Accuracy:

$$OA=\frac{Cc+Uu}{T}\times 100\% \tag{1}$$

OA describes the percentage of correct changed and unchanged detection pixels to the amount of testing samples.

● Kappa Coefficient:

$$\text{Kappa}=\frac{T(Cc+Uu)-(TC\times Tc+TU\times Tu)}{T^2-(TC\times Tc+TU\times Tu)} \tag{2}$$

Kappa Coefficient reveals the internal consistency of change detection results. It can describe detection accuracy more appropriately than overall accuracy.

● False detection ratio(Commission):

$$P_F=\frac{Cu}{TC} \tag{3}$$

It defines the percentage of false change caused by detection errors by using the ratio of false detected changes to total detected changes.

● Omission detection ratio:

$$P_0=\frac{Uc}{Tc} \tag{4}$$

It defines the percentage of omission change caused by detection errors by using the ratio of undetected changes to total true changes.

3 DATA AND STUDY AREA

Multi-temporal ALOS PRISM high spatial resolution data and AVNIR-2 multispectral data captured on December 23, 2006 and November 12, 2008 are used in this work for the change detection. All data are Level1 B2 products which are processed by primary radiometric and geometric corrections already. Linear regression model is used to atmospheric correction to the Level1 B2 data (Tang, *et al.*, 2004). For geometric correction, the multispectral images and panchromatic image are registered by the image to image mode using quadratic polynomial for coordinate transformation and bilinear interpolation for re-sampling, and the pixel errors were to 0.3 pixels. In order to combine the merits of panchromatic and multispectral images, *Principal Component Analysis* (PCA) fusion is used to generate the fused image dataset which contains both spatial and spectral information (Chavez, *et al.*, 1991).fusion is used to generate the fused image dataset which containing both spatial and spectral information.

In this paper, two case study areas are selected. Case area A is a square area around the Nanhu Campus of China University of Mining and Technology (CUMT) in the urban area of Xuzhou city, with size of 500×500 pixels in multi-spectral image corresponding to 2000×2000 pixels in the panchromatic image. Land cover changes in this study area during 2006 to 2008 are mainly composed of built-up areas and vegetation changes. Case study area B is Pangzhuang coal mining area located in the northwest of Xuzhou city with a size of 375×375 pixels in multi-spectral image corresponding to 1500×1500 pixels in the panchromatic image. Construction area, vegetation change and the rebuilt of subsiding areas are the main land cover changes in study area B during 2006 to 2008. Fig. 3 (a) shows the location of the two case areas with (b)—(c) and (d)—(e) are their false composite images of 2006 and 2008, respectively.

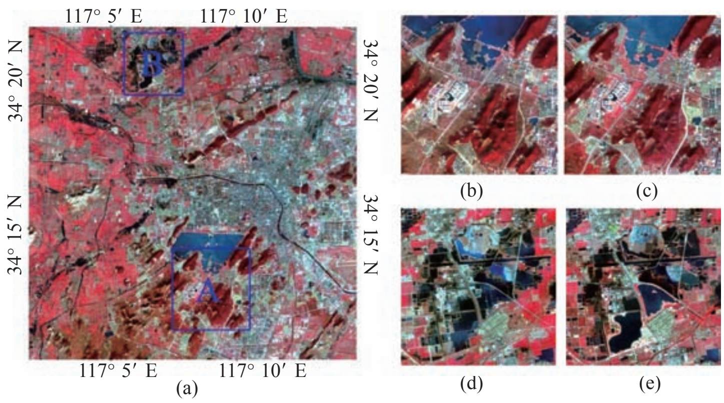

Fig. 3 Location of the case study areas and their false composite images
(a)Location of the two case areas; (b) Case area A 2006; (c) Case area A 2008; (d) Case area B 2006; (e) Case area B 2008

4 EXPERIMENTS AND ANALYSIS

4.1 Experiment on case study area A: urban area around CUMT

After comparing the change detection algorithms for different resolution data, unsupervised multi-band change detection method Change Vector Analysis (CVA) is used for the four-band ALOS multi-spectral image and fusion images and the supervised single-band change detection method *Support Vector Machine* (SVM) is applied in the ALOS panchromatic image. Then the coarse dataset detection result (500×500 pixels) is resampled into the same resolution with fine dataset result (2000×2000 pixels). Change areas are overlapped on the panchromatic image of year 2006 (Fig. 4), in which (a)—(c) represent the CVA change detection results of Ms data, SVM change map of Pan data and CVA results of Fusion data, respectively. According to the CTF decision fusion rules, final change intensity maps are generated by redefining all the pixels, as shown in Fig. 5 (a) (b).

In order to evaluate the results of different approaches, a group of change (3864 pixels) and unchanged (5892 pixels) test samples are selected as ground data based on the field work and image visual analysis. Then the confusion matrix (Table 4) is constructed to calculate the different change detection accuracy indexes.

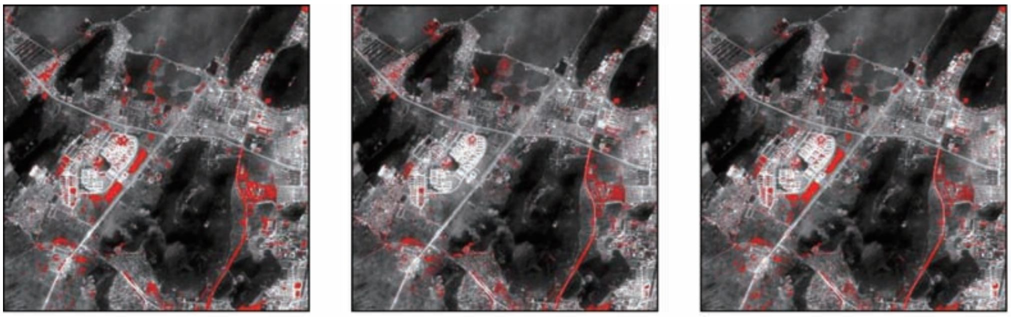

(a) (b) (c)

Fig. 4 Change maps of different datasets from different detection approaches
(a) CVA change map of MS data; (b) SVM change map of Pan data; (c) CVA change map of Fusion data

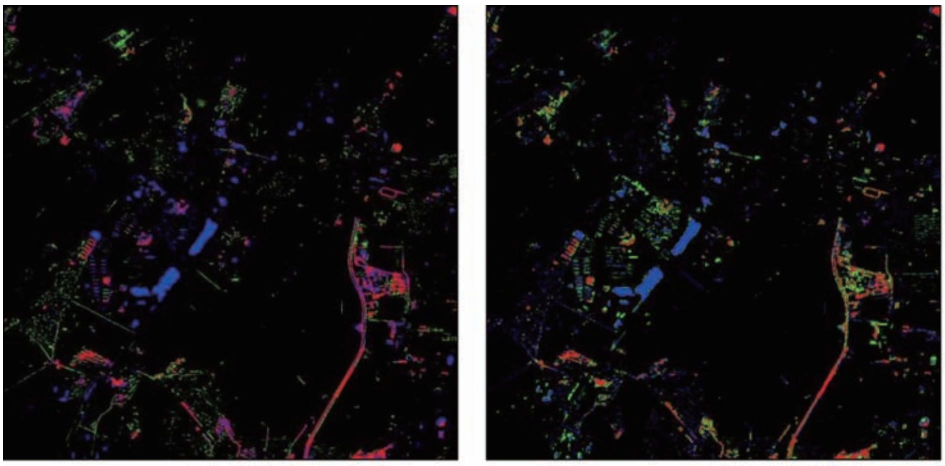

(a) (b)

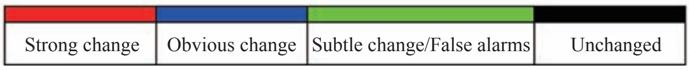

Fig. 5 Results of CTF detection based on decision level fusion
(a) Strategy 1 CTF fusion result; (b) Strategy 2 CTF fusion result

Table 4 Accuracy and errors of four change detection approaches

	Method/Accuracy	Overall Accuracy (OA)/%	Kappa	Omission/%	Commission/%
Coarse dataset (Ms)	CVA	81.00	0.6126	29.76	14.04
Fine dataset (Pan)	SVM	82.04	0.6347	25.50	15.40
Fine dataset (Fusion)	CVA	83.83	0.6721	23.03	13.55
Coarse to fine method	CTF fusion strategy 1	86.54	0.7288	15.28	14.13
	CTF fusion strategy 2	86.56	0.7274	19.66	10.60

Based on the accuracy of indicators listed in Table 4:

(1)The accuracy of the two CTF decision fusion strategies is higher than for a single dataset. Their overall accuracy and Kappa coefficient are 86.54% and 0.7288, 86.56% and 0.7274, respectively, which indicate an increase of 3—5 percentages than the single dataset detection results.

(2)The predominance of two CTF decision level fusion strategies is different. In strategy 1, only changes occurred in one dataset are viewed as final changes, which efficiently reduce the omission errors. Therefore, it has the lowest omission rate (15.28%) among all methods. Strategy 2 integrates the detection results of three datasets, changes occurred simultaneous in two or more datasets are regarded as final changes, and changes only appeared in one dataset are viewed as false alerts which will be abandoned. Therefore, the false alerts are restrained well, producing the lowest commission rate among all methods (10.60%). It can be shown that the proposed approach can combine the merits of different change detection algorithms and datasets obtains a more complete and comprehensive detection results.

(3)The defects of the two proposed strategies also cannot be ignored. The former one overlaps of the two datasets changes which will lead to a small increase of commission errors inevitably. However, the latter one will produce more omission errors because of the abandoning false alerts (occurred in only one dataset) which may contain a small amount of real change information. Therefore, according to the practical needs of the specific applications, the appropriate CTF fusion strategy should be selected in order to create the best detection results.

(4)For the results of a single dataset, *Fusion* data have the highest detection accuracy, indicating that by integration the spectral and spatial characteristics of multi-spectral and panchromatic data, the effect of change detection will be improved. Other remaining two single datasets have higher omission errors which lead to the poor performance of the overall detection accuracy.

Table 5 shows the ratios of different change intensity level areas to the total area using the two CTF fusion strategies. It can be seen that during 2006 to 2008 the change areas of study case area A occupy a 5%—7% of the total region area. Through redefining all pixels, the strong change areas occupy a 1.7%—1.82% of the total areas are simultaneity detected in different datasets, which can be set to the areas of maximized probability changes in the real scene. These strong change areas are the most important target of field work, and the obvious change areas can be considered as the important goal target of second periods of field work.

Table 5 Ratios of different change intensity levels

Method/Accuracy	Strong change/%	Obvious change/%	Subtle change/ False alarms/%	Unchanged/%	Total/%
CTF fusion strategy 1	1.82	2.14	1.47	94.57	100
CTF fusion strategy 2	1.70	2.41	3.29	92.60	100

An image block located in the campus of CUMT is chosen as the local analysis object to compare the performance of different CTF fusion strategies. Fig. 6 describes the changed areas of the regions from 2006 to 2008, in which the changed buildings are indicated by blue circles, and changed vegetation is indicated by red circles. The detailed ground change information obtained by field investigation are listed as: (1) library; (2) new student dormitory named as Xingyuan; (3) new refectory and dormitory; (4) new museum; (5—7) new man-made vegetation and green space.

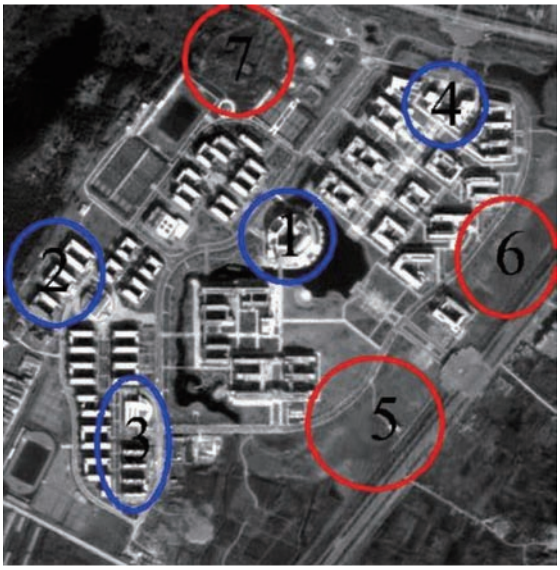

Fig. 6 Land cover changes in the Nanhu campus of CUMT from 2006 to 2008

Local detection results of three single image datasets and two CTF decision fusion strategies are shown in Fig. 7. It can be concluded that: (1) excepting some omission errors of vegetation in panchromatic dataset, most of real changes are detected effectively by all methods. Due to the lack of spectral information, single-band panchromatic data produces higher omission errors on vegetation changes; (2) both CTF strategies are effective in detecting the building change of the four locations where pixel intensity classified as strong change (areas in red), and vegetation change of three locations where classified into obvious change (areas in blue). Those results are completely consistent with filed work; (3) false alerts appeared in the experiment of CTF strategy 2 (areas in green) are mainly the detection errors of building shadows. Through the CTF decision fusion processing and removing these errors artificially, we can restrain the commission rate and improve the overall detection accuracy effectively; (4) from the local change results of a single dataset, the low resolution, incomplete structure of multi-spectral data, is inclined to cause a large number of commissions. Single-band panchromatic data lacking of spectral information will increase omission errors. *Fusion* dataset takes advantages of the former two dataset, but the new commission errors will be increased inevitably. Through the novel method proposed in this paper, the limitations of different single dataset will be improved, making the overall detecting results more consistent with the real changes.

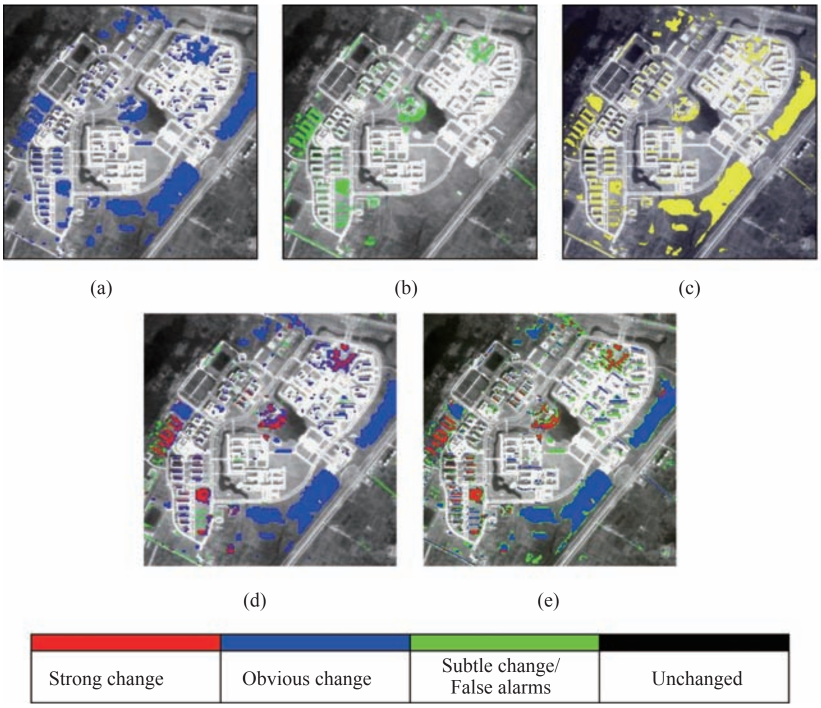

Fig. 7 Results of different methods experiments (detailed analysis on an image block)
(a)CVA change map of MS data; (b) SVM change map of Pan data; (c) CVA change map of Fusion data;
(d)Strategy 1 CTF fusion result; (e) Strategy 2 CTF fusion result

4.2 Experiment on case study area B: Pangzhuang mining area

In the experiment of case study area B, CVA is also used in detecting changes from multi-spectral coarse dataset and fusion fine dataset. SVM is selected to detect the change of the fine panchromatic dataset. Then the coarse dataset result (375×375) is resampled to the same spatial resolution with the results of the fine dataset (1500×1500). All the change results are overlapped on the panchromatic image of year 2006 (Fig. 8), which (a) — (c) represent the CVA change detection result of Ms data, SVM change map

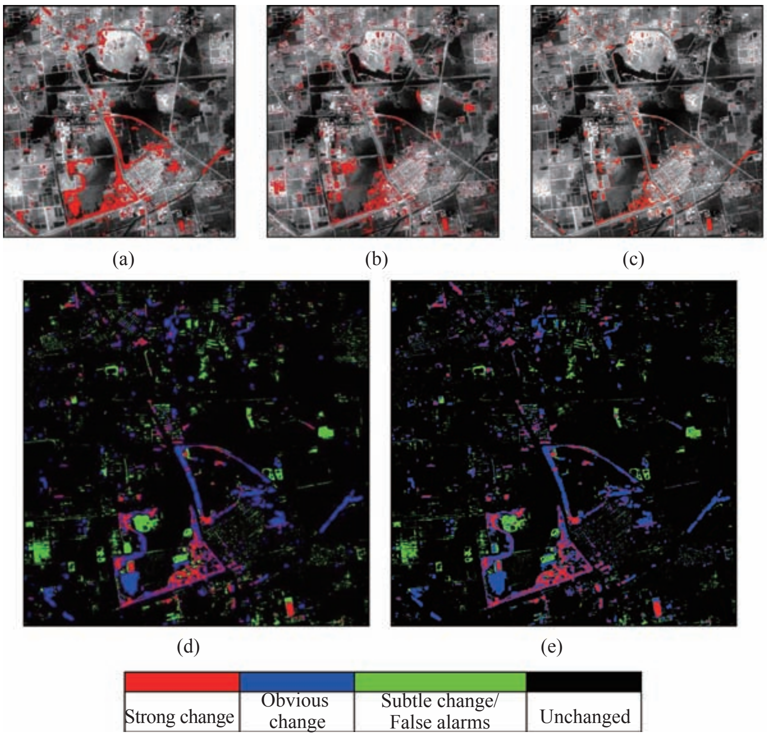

Fig. 8 Results of different change detection approaches
(a) CVA change map of MS data; (b) SVM change map of Pan data; (c) CVA change map of Fusion data;
(d) Strategy 1 CTF fusion result; (e) Strategy 2 CTF fusion result

of Pan data and CVA result of Fusion data, respectively. According to the CTF decision fusion rules, final change intensity maps are generated by combining change results of all three datasets, as shown in Fig. 8 (d) and (e).

A group of test samples including changed (2937 pixels) and unchanged (5172 pixels) pixels are selected as ground truth data to calculate the accuracy indices of different change detection methods, which are shown in Table 6.

Table 6 Accuracy and errors of four change detection approaches

	Method/Accuracy	Overall Accuracy(OA)/%	Kappa	Omission/%	Commission/%
Coarse dataset (Ms)	CVA	86.46	0.7060	26.09	10.50
Fine dataset (Pan)	SVM	85.99	0.6940	28.31	9.67
Fine dataset (Fusion)	CVA	86.85	0.7131	26.80	8.70
Coarse to fine method	CTF fusion strategy 1	90.65	0.8038	11.38	12.12
	CTF fusion strategy 2	89.67	0.7767	20.73	6.83

From the experimental results and the above table, we can summarize that:

(1)Two CTF fusion strategies have higher detection accuracy than any other single dataset, indicating that after decision level fusion, the proposed method integrates the merits of different datasets and different algorithms. It is an effective method that could be utilized in operational applications to improve the overall accuracy of change detection.

(2)CTF decision fusion effectively reduces the omission errors occurred in the single image dataset change detection, and increases the overall accuracy. Meanwhile, from the results it can be concluded that strategy 1 could well reduce the omission rate and strategy 2 could restrain the commission error effectively, which are consistent with the previous experimental results, confirming the feasibility and advantages of the proposed methods. However, in the practical utilization, the most appropriate CTF fusion strategy should be selected according to the application requirements, including omission minimized-oriented and/or commission minimized-oriented, to meet the needs of various applications.

(3)Due to the inherent characteristics of different single dataset, high omission rate is the main reason affects the final detection accuracy.

Ratios of different change intensity level areas to the total study areas are shown in Table 7. It can be seen that the change areas occupy nearly 10% in the case B total areas between year 2006 and 2008. After the change intensity reclassify, the strong changes occurred in all three datasets that occupy 1.82%—2.30% of the total area. These changes are mainly construction sites and vegetation changes in mining area according to investigation. Most of the obvious changes are the reconstruction of subsidence areas and vegetation of mining area. Those regions are also important targets in fieldwork.

Table 7 Ratios of different change intensity levels

Method/Accuracy	Strong change/%	Obvious change/%	Subtle change/ False alarms/%	Unchanged/%	Total/%
CTF fusion strategy 1	2.30	4.17	3.74	89.79	100
CTF fusion strategy 2	1.82	5.57	2.88	89.73	100

5 CONCLUSION

A novel change detection method based on CTF information processing and decision level fusion strategy is designed and proposed in this paper. Multi-temporal and multi-resolution ALOS remote sensing images are used in experiments to test its applicability in land cover change detection. Through this work, we can conclude that:

(1)The proposed decision level fusion change detection method for multi-resolution image data is demonstrated to be feasible and effective in land cover change detection. After integrating the results from different scales and different types of image datasets, the merits and characteristics of multiple datasets and algorithms are sound, which results in the better final detection result comparing to real land cover changes. Experimental results show that the proposed approach can remedy the limitations and uncertainty caused by a single dataset or a single detection algorithm, further narrowing and determining the change locations. Therefore, the new method could be of potential to be used in the practical land cover/use change detection tasks.

(2)Two CTF decision fusion strategies designed and experimented in this work have their own advantages. Strategy 1 can effectively reduce omission error, while strategy 2 performs well in restraining the commission error. According to the specific practical change detection applications, the appropriate strategy should be selected to obtain the most potential valuable change information, and then produces the most reliable change map in which the overall error is minimized.

(3)The proposed method converts the traditional “hard detection” into “soft detection”. Different level detection results are combining to realize the reclassifying of the change intensity step by step, which has more practical reference meaning and flexibility than simply separating all pixels into change and unchanged two classes. Moreover, the strong changes occurred in all datasets can be set as the maximum probability change areas, which are the most important detecting target areas of late land surveying and monitoring. Obvious changes occurred in most datasets are viewed as second place. Therefore, this approach will save labor cost and workload in field investigation process.

It should be noted that, according to the different characteristics and advantages and disadvantages of the two CTF fusion strategies, when using the proposed method we should consider the practical study areas and the datasets firstly. Further work will be focused on the selection of the most appropriate and effective detection algorithms for each single dataset, in order to make the change information more accurately. Meanwhile, how to minimize the omission error and commission error to improve the overall detection accuracy still needs to be analyzed further.

REFERENCES

Atiquzzaman M. 1999. Coarse-to-Fine search technique to detect circles in images. *The International Journal of Advanced Manufacturing Technology*, **15**(2): 96–102

Bovolo F and Bruzzone L. 2007. A theoretical framework for unsupervised change detection based on change vector analysis in the polar domain. *IEEE Transactions on Geoscience and Remote Sensing*, **45**(1): 218–236

Bruzzone L and Prieto D F. 2000. Automatic analysis of the difference image for unsupervised change detection. *IEEE Transactions on Geoscience and Remote Sensing*, **38**(3): 1171–1182

Castellana L, Addabbo A D and Pasquariello G. 2007. A composed supervised/unsupervised approach to improve change detection from remote sensing. *Pattern Recognition Letters*, **28**(4): 405–413

Chavez P S, Sides S C and Anderson J A. 1991. Comparison of three different methods to merge multiresolution and multis- pectral data: landsat TM and SPOT panchromatic. *Photogrammetric Engineering and Remote Sensing*, **57**(3): 295–303

Fung T and LeDrew E. 1987. Application of principal components analysis change detection. *Photogrammetric Engineering and Remote Sensing*, **53**: 1649–1658

Lambin E F and Strahlers A H. 1994. Change-vector analysis in multitemporal space: a tool to detect and categorize land-cover change processes using high temporal-resolution satellite data. *Remote Sensing of Environment*, **48**(2): 231–244

Li X, Hu W M and Hu W. 2006. A Coarse-to-Fine Strategy for Vehicle Motion Trajectory Clustering. Proceedings of the 18th International Conference on Pattern Recognition (ICPR'06), IEEE Computer Society Washington, DC, USA

Nemmour H and Chibani Y. 2006. Multiple support vector machines for land cover change detection: an application for mapping urban extensions. *ISPRS Journal of Photogrammetry and Remote Sensing*, **61**(2): 125–133

Riordan C J. 1981. Change detection for resource inventories using digital remote sensing data. Proceedings of the Workshop on In-Place Resource Inventories: Principles and Practices. Orono: University of Maine, 278–283

Sahbi H, Geman D and Boujemaa N. 2002. Face detection using coarse-to-fine support vector classifiers. Proceedings of the IEEE International Conference on Image Processing. New York: IEEE Computer Society Washington, DC: 925–928

Singh A. 1989. Review article digital change detection techniques using remotely-sensed data. *International Journal of Remote Sensing*, **10**(6): 989–1003

Sohl T L. 1999. Change analysis in the United Arab Emirates: an investigation of techniques. *Photogrammetric Engineering and Remote Sensing*, **65**(4): 475–484

Tang G A, Zhang Y S, Liu Y M, Xie Y L, Yang X and Liu A L. 2004. Remotely Sensed Digital Image Process. Beijing: Science Press: 111-112

Walter V. 2004. Object-based classification of remote sensing data for change detection. *ISPRS Journal of Photogrammetry and Remote Sensing*, **58**(3-4): 225–238

Woodcock C E, Macomber S A, Pax-Lenney M and Cohen W B. 2001. Monitoring large areas for forest change using Landsat: generalization across space, time and Landsat sensors. *Remote Sensing of Environment*. **78**(1–2): 194–203

决策级融合的多分辨率遥感影像变化检测

柳思聪[1]，杜培军[1,2]，陈绍杰[2]

1. 国土环境与灾害监测国家测绘局重点实验室 中国矿业大学，江苏 徐州 221116；
2. 龙岩学院 资源工程学院，福建 龙岩 364000

摘　要：针对多时相、多分辨率遥感影像数据的特点，充分考虑不同分辨率数据和不同变化检测应用的需求，将由粗到精数据集分层检测和决策级融合的思想引入到变化检测，以多时相多分辨率ALOS遥感影像为例，构建并试验了由粗到精变化检测的技术流程。该方法将ALOS多光谱数据视为粗数据集，将全色数据和融合数据视为精数据集，通过对3种数据集变化检测结果按照一定的决策规则进行综合，生成最终的变化检测结果图，反映变化的发生位置及变化强度。选择江苏省徐州市城区和矿区两个区域进行试验并与常规变化检测算法结果进行对比，表明该方法具有更好的检测效果，可以有效地应用于多分辨率遥感影像变化检测，并为实际野外调查提供重要的检测靶区。

关键词：变化检测，由粗到精，决策级融合，土地覆盖变化

中图分类号：TP75　　**文献标志码**：A

引用格式：柳思聪，杜培军，陈绍杰．2011．决策级融合的多分辨率遥感影像变化检测．遥感学报，**15**(4): 846–862
Liu S C, Du P J and Chen S J. 2011. A novel change detection method of multi-resolution remotely sensed images based on the decision level fusion. *Journal of Remote Sensing*, **15**(4): 846–862

1 引　言

多时相遥感影像的变化检测一直以来在遥感应用当中扮演着重要的角色，其应用涵盖土地利用/覆盖变化、森林和植被变化以及城市扩展和灾害监测等领域。变化检测的实质是通过观测一个物体或者现象在不同时间下的状态以识别出变化(Singh, 1989)。近几十年来，国内外专家学者相继提出和发展了多种变化检测的方法，使得变化检测的手段更为丰富。对于二值变化检测(Binary Change Detection)来说，目前常规的变化检测方法可以分为两大类：监督变化检测和非监督变化检测。前者类似于监督分类，需要事先获得合适的训练样本输入检测模块从而进行检测，如分类后比较、人工神经网络和支持向量机等方法(Castellana等, 2007; Nemmour和Chibani, 2006; Woodcock等, 2001)。后者不需要获得先验样本，直接对原始影像进行分析和处理，获得变化信息，如图像差值阈值法、图像比值法、变化矢量分析法、主成分变化法和面向对象方法(Bovolo和Bruzzone, 2007; Bruzzone和Prieto, 2000; Fung和LeDrew, 1987; Lambin 和 Strahler, 1994; Riordan, 1981; Sohl, 1999; Walter, 2004)等。所有这些变化检测方法都在不同的研究中显示出可用性和优越性。但是，对于遥感影像变化检测来说，还面临以下问题需要解决：首先，不同变化检测方法适用性不同，有的适用于单波段检测，有的适用于多波段检测，没有任何一种普遍适用的高精度方法；其次，不同尺度的遥感数据源所包含的信息大为不同，特别是对于同一卫星下多分辨率影像数据来说，多光谱数据丰富的光谱信息和全色数据良好的空间分辨率及纹理信息对于不同方法的检测结果影响很大；再次，不同应用目的的变化检测对于漏检和虚检率要求不同，如何着眼于具体应用，选择具有最小漏检率或者是最小虚检率的变化检测方法，最大限度满足变化检测

收稿日期：2010-03-22；**修订日期**：2010-06-20

基金项目：国家高技术研究发展计划(863计划)(编号：2007AA12Z162)，国家自然科学基金(编号：40871195)和江苏省“333工程”科研项目(编号：2009-32)

第一作者简介：柳思聪(1986－)，男，硕士研究生，研究方向为遥感图像处理与遥感应用。E-mail：allencong@163.com。

通信作者：杜培军，E-mail: dupjrs@126.com。

的需求还未得到广泛研究。

针对这些问题，本文将由粗到精(Coarse to fine，CTF)多分辨率图像处理、决策树、决策级融合(Decision Level Fusion)等方法理论引入多时相多分辨率遥感影像的变化检测，针对降低漏检率和抑制虚检率两种具体应用需求设计了两种基于决策级融合的变化检测方法，并比较其与常规方法的检测结果，以探求方法的可行性和适用性。不同于常规由粗到精理论的定义，本文方法主要针对多分辨率遥感影像数据下不同分辨率数据集进行不同层次的变化检测，通过对不同尺度数据源和不同类型变化检测方法的结果进行集成，充分利用不同方法和不同数据集的优势，从而避免和减少使用单一方法和单一数据源进行检测时的不确定性和限制。

2 多分辨率数据由粗到精决策级融合的变化检测方法

通常，由粗到精理论主要被用于模式识别领域，如人脸识别与检测、移动车辆轨迹检测和图像形状检测等(Atiquzzaman, 1999; Li 等, 2006; Sahbi 等, 2002)。在遥感影像处理领域，由粗到精的思想多用于多尺度遥感影像的处理过程，特别在对于同一遥感卫星所获取的全色和多光谱数据的处理中尤为有效。本文提出的由粗到精决策级融合的变化检测方法利用不同尺度和类型的数据集和不同变化检测方法的优势及特点，综合性地检测变化的发生位置并且定义变化的强度，其中变化强度最大的区域可视为实际野外勘察的目标靶区。同时，设计和试验两种针对不同应用的由粗到精(CTF)融合规则，以最大限度的降低漏检率，抑制虚检率，从整体上提高变化检测的精度。

方法的具体流程图如图1所示。具体针对本文所使用的ALOS影像数据，设计和试验两种CTF融合的变化检测方案，具体步骤如下：

方案1：

(1)将10 m分辨率的ALOS多光谱(Multi-spectral，Ms)影像视为粗数据集，将2.5 m分辨率的全色(Panchromatic，Pan)影像视为精数据集。然后分别对两种数据集进行不同变化检测方法的试验；

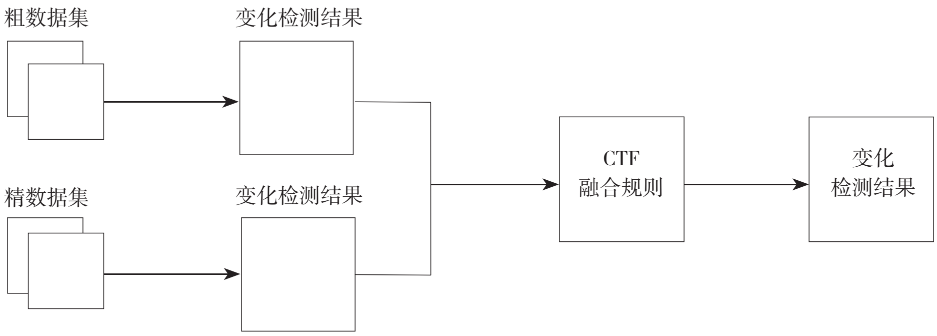

图1　基于决策级融合的由粗到精变化检测方法流程

(2)求出两种数据集的变化检测结果图，并将其重采样至同一分辨率；

(3)建立CTF决策融合规则将两种数据集检测结果融合成一幅变化强度图，并将所有像元划分定义成4类：强烈变化(变化同时发生在两种数据集上)，明显变化(粗数据集上发生变化而精数据集上不发生变化)，细微变化(精数据集上发生变化而粗数据集上不发生变化)和不变化。

表1为最终所有像元变化强度的定义表，其中粗数据集和精数据集检测结果中变化的像素和非变化像素的值分别用1和0表示。图2为根据变化强度表建立的决策树规则，其中B1代表精数据集的检测结果，B2代表粗数据集的检测结果。

表1　像元变化强度定义表

数据类型	像素值			
精数据集	1	0	1	0
粗数据集	1	1	0	0
变化强度	强烈变化	明显变化	细微变化	不变化

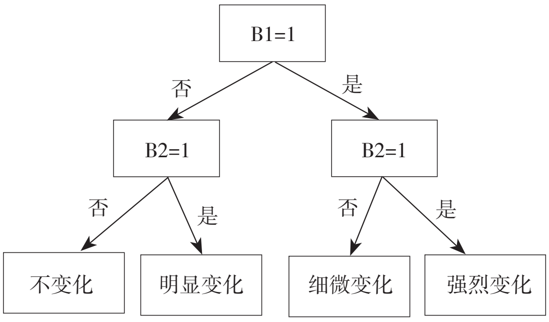

图2 由粗到精变化检测法决策树规则

方案2：

(1)将ALOS多光谱影像视为粗数据集，全色和融合(Fusion)影像视为精数据集，分别对3种数据进行变化检测；

(2)将粗数据集检测结果采样至与精数据集同一分辨率；

(3)建立CTF决策融合规则：强烈变化(变化同时出现在3种数据集上)，明显变化(变化同时出现在两种数据集上)，虚假变化(变化只出现在1种数据集上)和不变化。最后将前两者作为最终变化区域，后两者作为不变化。表2为最终所有像元变化强度的定义表。

表2 像素变化强度定义表

数据类型	像元值							
粗数据集(Ms)	1	1	1	0	1	0	0	0
精数据集(Pan)	1	1	0	1	0	1	0	0
精数据集(Fusion)	1	0	1	1	0	0	1	0
变化强度	强烈变化	明显变化			虚检变化(不变化)			不变化

对变化检测结果的精度评价一般参考遥感影像分类的精度评定方法，即构造误差矩阵(也称混淆矩阵，Confusion Matrix)计算相关精度指标，如表3所示。

表3 变化误差矩阵

变化检测结果/验证数据	实际变化像元(c)	实际非变化像元(u)	总和(T)
检测到的变化像元(C)	Cc	Cu	TC
检测到的非变化像元(U)	Uc	Uu	TU
总和(T)	Tc	Tu	T

通常定义以下几种评价变化检测的指标：

●总体检测精度(Overall Accuracy)：

$$OA=\frac{Cc+Uu}{T}\times 100\% \tag{1}$$

表示检测正确的样本数占总样本数的比率，反映了总体的检测准确度。

●Kappa系数(Kappa Coefficient)：

$$\text{Kappa}=\frac{T(Cc+Uu)-(TC\times Tc+TU\times Tu)}{T^2-(TC\times Tc+TU\times Tu)} \tag{2}$$

Kappa系数表示了检测结果内部的一致性，比OA更客观地反映检测结果的精度。

●虚检率(Commission error)：

$$P_{虚检}=\frac{Cu}{TC} \tag{3}$$

表示检测误差引起的虚假变化的概率。

●漏检率(Omission error)：

$$P_{漏检}=\frac{Uc}{Tc} \tag{4}$$

表示检测误差产生的漏检变化的概率。

3 试验数据和研究区

试验使用ALOS遥感卫星影像的可见光近红外多光谱影像(AVNIR-2)和全色数据(PRISM)。影像获取时间是2006-12-23和2008-11-12。图像获取时间都为11月—12月(即秋冬季)，地物覆盖类别信息较一致，便于进行变化检测。使用的ALOS数据均为Level1 B2级数据，已经过初步的辐射与几何校正。在此基础上，运用线性回归分析法进行辐射精校正(汤国安 等, 2004)，通过影像对影像模式进行几何精校正。由二次多项式法进行坐标变换，采用双线性内插法进行灰度值重采样，最后匹配精度控制在0.3个像元之内。对两个时相的全色影像和多光谱影像分别应用主成分分析(Principal Component Analysis，PCA)算法进行融合(Chavez等, 1991)，以充分利用两种数据集，最大限度保持光谱和纹理信息。

根据研究区的实际情况和图像所覆盖的范围采取两个区域作为试验对象，其中研究区A位于徐州市泉山区，主要包括了云龙湖的小南湖部分，中国矿业大学南湖校区、泉山和云龙山等主要地物，对应于多光谱影像上500×500像元大小，全色影像上

2000×2000像元范围的区域。研究区A在2006年—2008年土地覆盖变化主要为城市建设用地及植被的变化，包括中国矿业大学南湖校区、铜山新区商品房和政府安置房的建设及云龙湖小南湖的改建工程等；研究区B位于徐州市西北部的庞庄煤矿，对应于多光谱影像上375×375像元和全色影像上1500×1500像元范围。研究区B在2006年—2008年间变化主要包括矿区建筑物的变化、植被变化和塌陷地的综合整治工程等。图3(a)为两个研究区域所处的位置，图3(b)—(c)和(d)—(e)分别为研究区A和B 2006年及2008年ALOS多光谱影像432波段的假彩色合成影像。

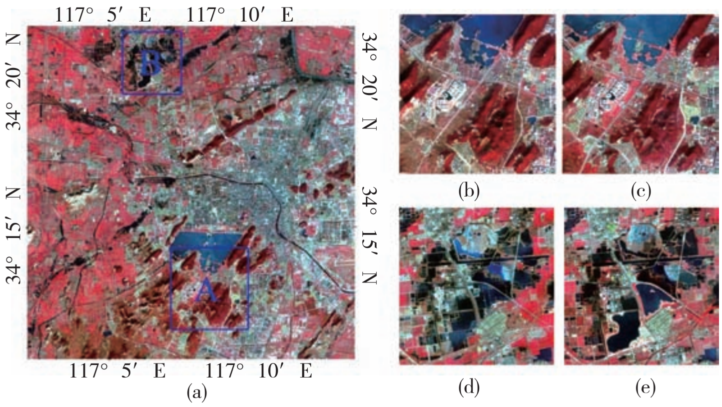

图3 研究区A和B位置及两时相ALOS假彩色合成影像

(a)研究区位置；(b)2006年研究区A；(c)2008年研究区A；(d)2006年研究区B；(e)2008年研究区B

4 实验结果与精度评价

4.1 研究区A试验(城区)

通过对不同分辨率数据常规变化检测算法的应用效果比较，对两个时相4波段ALOS多光谱影像和融合影像选用经典多波段变化检测法变化矢量方法(Change Vector Analysis，CVA)方法；对ALOS全色影像选用单波段监督变化检测法支持向量机(Support Vector Machine，SVM)方法。然后将粗数据集检测结果(500×500像元)重采样至与精数据集同样分辨率(2000×2000像元)，检测的变化结果叠加显示在2006年全色波段上(图4)，其中图4(a)—(c)分别为多光谱数据的CVA检测结果、全色数据SVM检测结果和融合数据CVA检测结果。

根据建立的CTF决策融合规则，将不同数据集的检测结果融合生成最终变化强度图，并对最终的变化区域进行强度定义，如图5(a)(b)所示。

为评价不同检测方法的结果，在实地考察和对影像可视化分析的基础上，选取一组图像上变化(3864个像元)与不变化(5892个像元)的样本数据，将其视为真实地面数据，从而构造混淆矩阵(表4)，计算不同方法的检测精度指标。

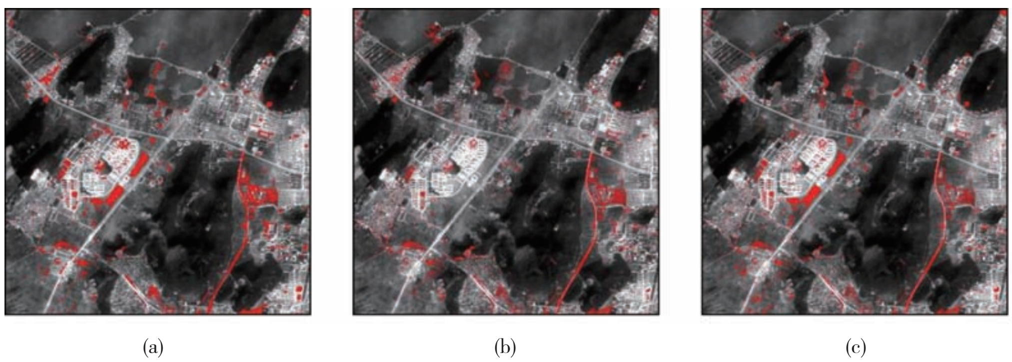

图4 不同影像数据集的检测结果

(a) 粗数据集Ms影像CVA检测结果；(b) 精数据集Pan影像SVM检测结果；(c) 精数据集Fusion影像CVA检测结果

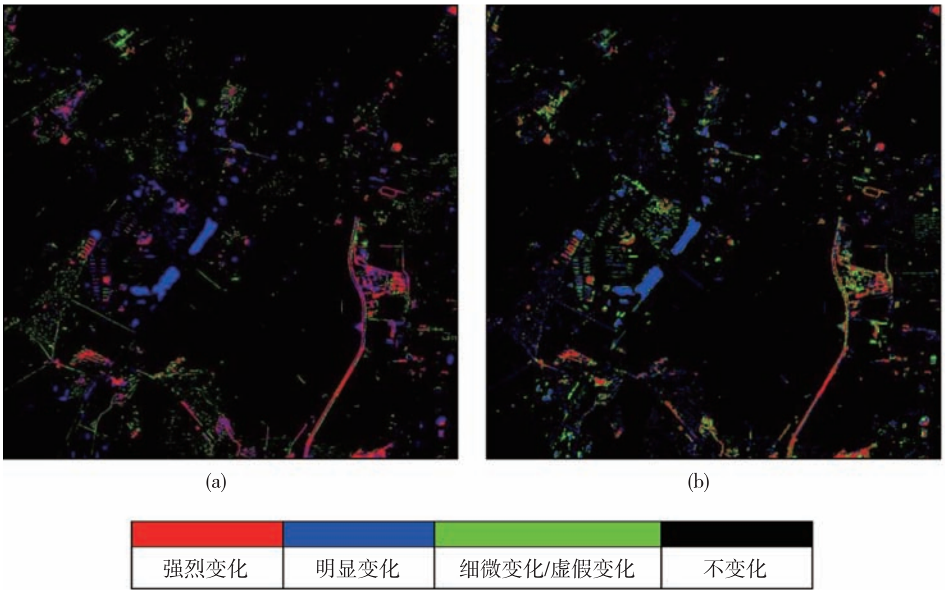

图5 由粗到精决策级融合方法检测结果
(a) 方案一检测结果；(b) 方案二检测结果

表4 变化检测精度及误差

	方法/精度	总体精度(OA)/%	Kappa	漏检率/%	虚检率/%
粗数据集(Ms影像)	CVA	81.00	0.6126	29.76	14.04
精数据集(Pan影像)	SVM	82.04	0.6347	25.50	15.40
精数据集(Fusion影像)	CVA	83.83	0.6721	23.03	13.55
由粗到精方法	CTF融合方案1	86.54	0.7288	15.28	14.13
	CTF融合方案2	86.56	0.7274	19.66	10.60

从表中可以看出：

(1)两种决策级融合的变化检测方法精度都优于单一数据集影像的检测精度。两种方案总体精度和Kappa系数分别达到86.54%和0.7288，86.56%和0.7274，在单一数据检测结果基础上提高近3%—5%。

(2)两种决策级融合方法各具优势。方案1CTF融合规则，将只出现在单一数据集上的变化视为变化区域，很好地降低了漏检误差，其漏检率在所有方法中最低仅为15.28%；方案2CTF融合规则集成了3种数据影像集检测结果，将出现在两种及两种以上数据集中的变化视为最终变化，只出现在1种数据集上的变化视为虚检变化予以舍弃，很好地抑制了虚检误差，其虚检率仅为最低的10.60%。这说明由粗到精方法集成了不同检测方法对于不同数据集变化检测的优势，使得检测结果更加完整与全面。

(3)两种CTF方案稍有不足在于，前者对于两种数据集变化的叠加会不可避免导致少量虚检的增加，后者因为舍弃的虚检变化部分可能包含少量真实变化信息，又造成一些新的漏检产生。所以具体应用时应根据实际需求，选择合适的CTF融合方案，以获得最佳的检测结果。

(4)对于单一数据集的检测结果中，融合影像的检测精度最高，说明其集成和互补了多光谱和全色数据在光谱和空间的优势，提高了变化检测的效果。其余两种影像数据较多的漏检变化导致整体检测效果不佳。

表5为两种CTF融合方案检测结果得到的变化强度等级面积占总面积的比例。从表中可以看出，研究区A在2006年—2008年间变化地物面积占区域总面积的5%—7%，通过变化强度的分级，其中强烈变化面积占研究区总面积的1.7%—1.82%，这部分区域的变化在不同数据集上同时被检测到，可设定为实地发生变化可能性最大的区域。因此在野外勘察及相关工作时可作为首要的检测靶区。变化强度居次的明显变化可作为第2阶段野外考察重要的目标靶区。

表5 不同变化强度等级面积比例 /%

方法/变化强度	强烈变化	明显变化	细微变化	不变化	总计
CTF融合方案1	1.82	2.14	1.47	94.57	100
CTF融合方案2	1.70	2.41	3.29	92.60	100

为对比和分析由粗到精检测不同方法组合的局部检测效果，在图像上裁取了中国矿业大学南湖校区主要部分的一小块图像作为局部分析对象。图6在2008年全色影像上标识了2006年—2008年南湖校区实际地物变化的位置，图上变化主要包括建筑物和植被两类，其中变化的建筑物用蓝色圈出，变化的植被用红色圈出。

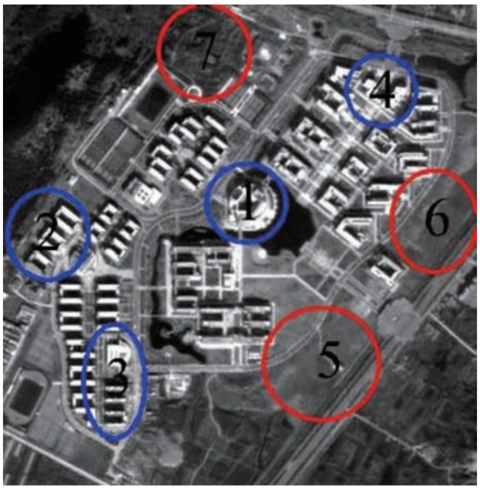

图6 2006年—2008年中国矿业大学南湖校区实际地物变化示意图。

变化位置1为校图书馆，2为新建的学生公寓—杏苑，3为新建的学生3食堂和研究生公寓，4为新建的中国煤炭科技博物馆。5—7红色圈出的位置都为学校人工绿化的新增区域。

图7所示为3种单一影像数据集和两种CTF决策融合检测方法试验的局部检测结果。从图上可以看出：(1)除了全色影像上部分植被的漏检，其余不同检测方法都较为有效地检测到了实地大部分的变化区域。单波段全色数据因为缺乏较多的光谱信息，导致对于植被变化的漏检；(2)两种CTF方案都有效地检测到了4个位置的建筑物变化，将其像元强度等级划为强烈变化(图中红色部分)，同时也有效检测到了3处植被的变化，将其划为明显变化(图中蓝色部分)，这与实地考察结果相一致；(3)CTF方案2试验中出现的虚检变化(图中绿色部分)主要为对于建筑物阴影的错检，通过CTF决策融合，人为去除了这部分虚检，有效抑制了虚检率，提高了整体检测精度；(4)从单一影像数据集局部检测结果来看，多光谱数据分辨率低、结构不完整，容易出现大量虚检，全色单波段精数据集缺乏丰富的光谱信息，容易造成漏检变化，而融合影像虽然利用前两者的优势，但是不可避免会带入新的虚检增加。而通过本文方法则很好地弥补了不同数据集的缺陷，使得整体检测结果与实地变化更为一致。

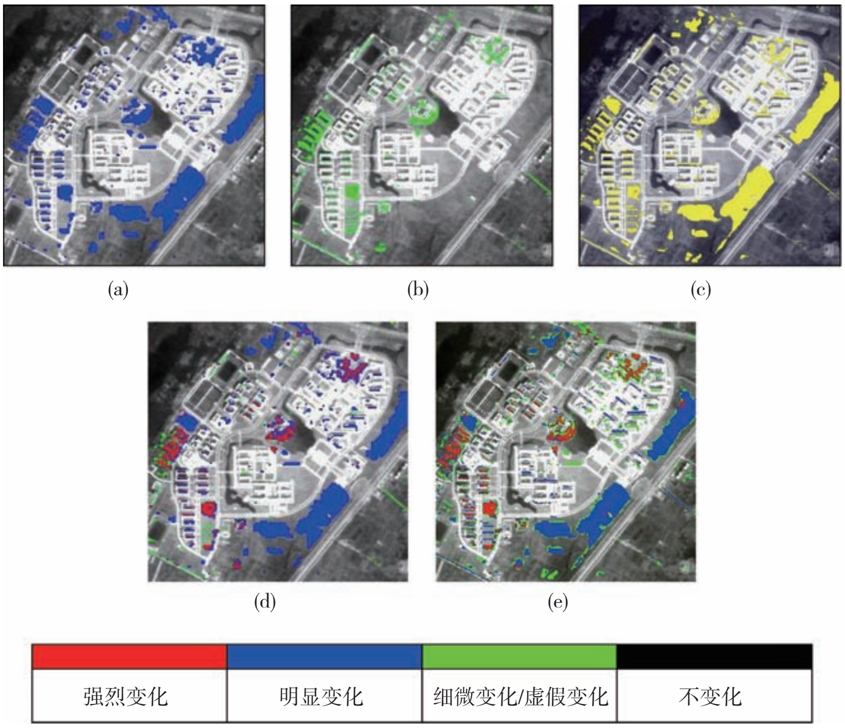

图7 不同变化检测方法试验局部检测结果

(a)粗数据集Ms影像CVA检测结果；(b) 精数据集Pan影像SVM检测结果；(c) 精数据集Fusion影像CVA检测结果；(d) 方案1CTF融合检测结果；(e) 方案2CTF融合检测结果

4.2 研究区B试验(矿区)

对研究区B的试验，同样使用CVA方法检测多光谱粗数据集和融合影像精数据集的变化；使用SVM方法检测全色影像精数据集的变化；然后将粗数据集检测结果(375×375像元)重采样至与精数据集同样分辨率(1500×1500像元)，检测的变化结果叠加显示在2006年全色波段上(图8)，图8(a)—(c)分别为多光谱数据的CVA检测结果、全色数据SVM检测结果和融合数据CVA检测结果。

根据两种CTF决策融合规则，将不同数据集的检测结果融合生成最终变化强度图(图8(d)(e))。

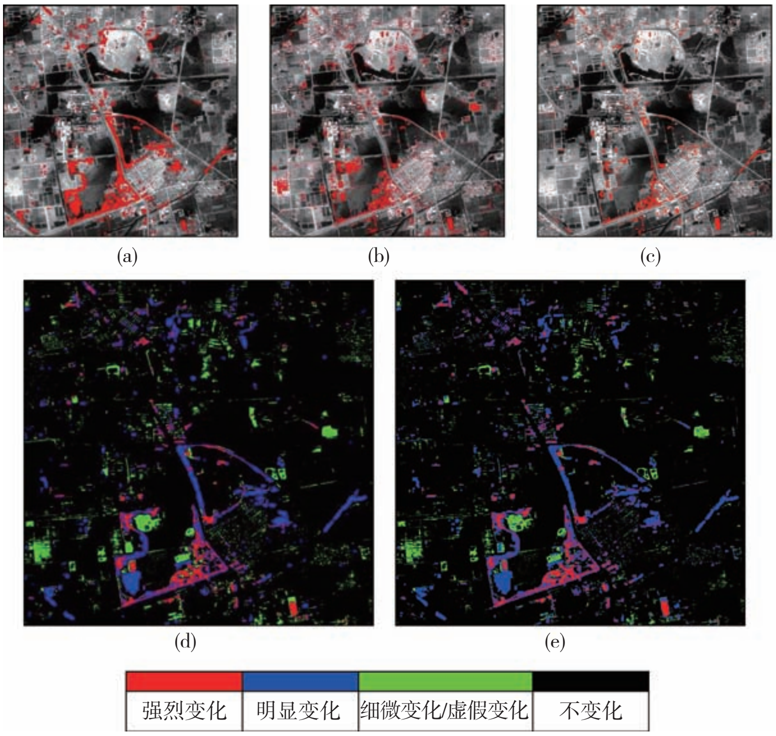

图8　不同变化检测方法结果

(a)粗数据集Ms影像CVA检测结果；(b) 精数据集Pan影像SVM检测结果；(c) 精数据集Fusion影像CVA检测结果；(d) 方案1检测结果；(e) 方案2检测结果

参照前一试验，选取图像上变化(2937个像元)与不变化(5172个像元)的样本数据，将其视为真实地面数据，构造混淆矩阵计算不同方法的检测精度指标(表6)。

从试验结果和表中可以看出：

(1)两种CTF融合方法的检测精度都比其余任何1种单一数据集检测结果要高，这说明该方法通过决策融合，集中了不同数据集和不同方法的优势，在现实中是切实可行的，且可以有效提高检测的效果。

(2)通过CTF融合，有效弥补了在单一影像数据集检测中出现的大量漏检变化，使得整体检测精度得到提高。同时，由试验结果来看，方案1可以有效降低漏检率，方案2可以有效抑制虚检率，这与前一试验结果相一致，也进一步验证了方法的可行性与优势。

表6　变化检测精度及误差

	方法/精度	总体精度(OA)/%	Kappa	漏检率/%	虚检率/%
粗数据集(Ms影像)	CVA	86.46	0.7060	26.09	10.50
精数据集(Pan影像)	SVM	85.99	0.6940	28.31	9.67
精数据集(Fusion影像)	CVA	86.85	0.7131	26.80	8.70
由粗到精方法	CTF融合方案1	90.65	0.8038	11.38	12.12
	CTF融合方案2	89.67	0.7767	20.73	6.83

在具体现实应用时，可根据具体应用需求，选择合适的CTF融合策略，从最大限度降低漏检率和最大限度抑制虚检率两个方面加以选择，以满足实际检测的需要。

(3)对单一数据集的检测当中，由于不同数据集的自身特点，较高的漏检率是影响其最终检测精度的主要原因。

表7为不同方法组合的由粗到精变化检测的变化强度等级面积占总面积的比例。可以看出，研究区B在2006年—2008年间变化地物面积占区域总面积的10%左右，通过变化强度的分级，同时在3种影像数据集上被检测到的强烈变化像元面积占研究区总面积的1.82%—2.30%，经实地考察主要为矿区建设用地和矿区植被等的变化。明显变化部分主要为矿区塌陷地积水区改建和植被等的变化，这些区域也是野外考察的重要目标靶区。

表7　不同变化强度等级面积比例　/%

方法/变化强度	强烈变化	明显变化	细微变化	不变化	总计
CTF融合方案1	2.30	4.17	3.74	89.79	100
CTF融合方案2	1.82	5.57	2.88	89.73	100

5　结　论

在设计和构造由粗到精变化检测思想和不同影像数据集检测结果决策融合的基础上，利用多时相多分辨率的ALOS遥感影像，实验对比分析了其在变化检测中的适用性和检测效果。通过研究，可以得到以下结论：

(1)本文提出的针对多分辨率数据决策级融合的变化检测方法在土地覆盖变化检测的实际应用中是可行且有效的。通过融合不同尺度不同类型遥感数据集的检测结果，充分利用了不同数据集和不同方法的特点和优势，使得最终检测结果更加趋近于实际变化。试验证明，该方法很好地弥补了由于单一数据集或者是单一检测方法所带来的局限性和不确定性，更进一步缩小和确定了实地变化发生的位置，可以在现实的土地变化检测中推广和使用。

(2)设计和试验的两种由粗到精决策融合方案分别具有不同优势，方案1可有效降低漏检变化，方案2优势在于抑制虚检变化，具体在实际变化检测应用当中，可针对不同需求选择合适方案，以获得最大价值的变化检测信息。

(3)由粗到精方法将传统意义上的“硬检测”转变为“软检测”，通过不同层次的检测结果综合，逐步实现对所有像元的变化强度等级划分。这比单纯地将像元分为变化和非变化两类更具有实际参考价值和灵活性。检测结果中，同时发生在多个数据集上的强烈变化是实地最大可能发生变化的区域，可作为后期土地勘察和执法当中首要的检测靶区，而发生在多个数据集上的明显变化等区域次之。这就为实际外业调查过程节省了大量资源和工作量。

应该指出的是，根据两种CTF融合策略各自不同的特点和优缺点，在实际的研究和方法使用当中，还应视研究区域和所使用数据的实际情况选择应用。同时，对不同的数据集分别选择最适用的检测方法进行由粗到精融合，从而更精确地获得变化信息，提高检测效果，同时最大限度地抑制虚检和漏检变化的发生，将是今后工作的重点。

REFERENCES

Atiquzzaman M. 1999. Coarse-to-Fine search technique to detect circles in images. *The International Journal of Advanced Manufacturing Technology*, **15**(2): 96–102

Bovolo F and Bruzzone L. 2007. A theoretical framework for unsupervised change detection based on change vector analysis in the polar domain. *IEEE Transactions on Geoscience and Remote Sensing*, **45**(1): 218–236

Bruzzone L and Prieto D F. 2000. Automatic analysis of the difference image for unsupervised change detection. *IEEE Transactions on Geoscience and Remote Sensing*, **38**(3): 1171–1182

Castellana L, Addabbo A D and Pasquariello G. 2007. A composed supervised/unsupervised approach to improve change detection from remote sensing. *Pattern Recognition Letters*, **28**(4): 405–413

Chavez P S, Sides S C and Anderson J A. 1991. Comparison of three different methods to merge multiresolution and multis- pectral data: landsat TM and SPOT panchromatic. *Photogrammetric Engineering and Remote Sensing*, **57**(3): 295–303

Fung T and LeDrew E. 1987. Application of principal components analysis change detection. *Photogrammetric Engineering and Remote Sensing*, **53**: 1649–1658

Lambin E F and Strahlers A H. 1994. Change-vector analysis in multitemporal space: a tool to detect and categorize land-cover change processes using high temporal-resolution satellite data. *Remote Sensing of Environment*, **48**(2): 231–244

Li X, Hu W M and Hu W. 2006. A Coarse-to-Fine Strategy for Vehicle Motion Trajectory Clustering. Proceedings of the 18th International Conference on Pattern Recognition (ICPR'06), IEEE Computer Society Washington, DC, USA

Nemmour H and Chibani Y. 2006. Multiple support vector machines for land cover change detection: an application for mapping urban extensions. *ISPRS Journal of Photogrammetry and Remote Sensing*, **61**(2): 125–133

Riordan C J. 1981. Change detection for resource inventories using digital remote sensing data. Proceedings of the Workshop on In-Place Resource Inventories: Principles and Practices. Orono: University of Maine, 278–283

Sahbi H, Geman D and Boujemaa N. 2002. Face detection using coarse-to-fine support vector classifiers. Proceedings of the IEEE International Conference on Image Processing. New York: IEEE Computer Society Washington, DC: 925–928

Singh A. 1989. Review article digital change detection techniques using remotely-sensed data. *International Journal of Remote Sensing*, **10**(6): 989–1003

Sohl T L. 1999. Change analysis in the United Arab Emirates: an investigation of techniques. *Photogrammetric Engineering and Remote Sensing*, **65**(4): 475–484

Tang G A, Zhang Y S, Liu Y M, Xie Y L, Yang X and Liu A L. 2004. Remotely Sensed Digital Image Process. Beijing: Science Press: 111-112

Walter V. 2004. Object-based classification of remote sensing data for change detection. *ISPRS Journal of Photogrammetry and Remote Sensing*, **58**(3-4): 225–238

Woodcock C E, Macomber S A, Pax-Lenney M and Cohen W B. 2001. Monitoring large areas for forest change using Landsat: generalization across space, time and Landsat sensors. *Remote Sensing of Environment*. **78**(1–2): 194–203

附中文参考文献

汤国安, 张友顺, 刘咏梅, 谢元礼, 杨昕, 刘爱利. 2004. 遥感数字图像处理. 北京: 科学出版社, 111–112